Four-Wave Mixing in a Multi-Layer SiN_x/a-Si:H Photonic Chip

Michael Kossey, Kangmei Li, Hongcheng Sun, Amy C. Foster
Department of Electrical and Computer Engineering, Johns Hopkins University, Baltimore, MD 21218, USA
amy.foster@jhu.edu

Abstract: We demonstrate four-wave mixing (FWM) in a-Si:H waveguides in a multi-layer integrated photonic chip. The a-Si:H waveguides are accessed through interlayer couplers from waveguides composed of SiN_x and exhibit 0.45±0.05 dB loss per transition.

OCIS codes: (130.3120) Integrated optics devices; (220.4241) Nanostructure fabrication; (230.4320) Nonlinear optical devices

1. Introduction

Integrated photonics has enabled a wealth of exciting device demonstrations ranging from integrated frequency combs to heralded single photons. The functionality of every photonic device relies upon specific material properties including propagation loss, electrical characteristics, nonlinearity, and band-gap to name just a few. Every material provides its own advantages and disadvantages. For example, silicon nitride (SiN_x) can form ultra-low propagation loss waveguides [1] but has a relatively small nonlinear refractive index [2], while amorphous silicon (a-Si:H) has excellent nonlinearity but modest propagation losses [3]. As individual photonic devices are combined to make multifunctional systems, the demands on material properties become greater and greater until no single material can fulfill all requirements. The optimal solution to this problem is using a heterogeneous material platform, in which an optical signal could move from material to material as different properties become desirable, and can allow for an entire optical system to be built on a single chip. Such an approach has been integral in creating on-chip laser sources on silicon platforms [4].

In a heterogeneous material platform, different materials are present in different layers vertically offset from each other. Because most fabrication of integrated photonic devices is based on photolithography, a two-dimensional process, specialized structures such as interlayer couplers are required to move light out of plane to shift from one material to another. Two primary approaches to interlayer coupling exist. The first uses pairs of grating couplers to diffract light out of and back into plane [5,6]. However, the use of gratings imposes a bandwidth limit on the interlayer coupler, and grating directionality can lead to interlayer crosstalk unless tightly controlled. The second approach is based on evanescent coupling [7–9]. Simply positioning two waveguides near each other in two different layers of material will allow light to couple from one layer to another, provided the mode fields of the two are close enough to interact. This approach has a much simpler design, making fabrication less complicated, and can also have a much larger bandwidth than a grating-based approach. While the interaction length of the evanescent coupler can be large, the advantages made it our approach of choice in this work.

2. Design and Fabrication

We choose the materials SiN_x and a-Si:H for our heterogeneous material platform because, as discussed above, the two materials illustrate the tradeoff between propagation loss and nonlinearity. The waveguide dimensions in the two materials are 2.5 μm x 260 nm for SiN_x and 320 nm x 240 nm for a-Si:H. Both waveguides are clad in silicon dioxide. We select a vertical separation of 700 nm between the two layers. Based on finite-difference method (FDM) simulation, we find that tapering the two waveguides down to and up from widths of 150 nm over a length of 300 μm results in >99% transmission at a wavelength of 1550 nm.

a) b)

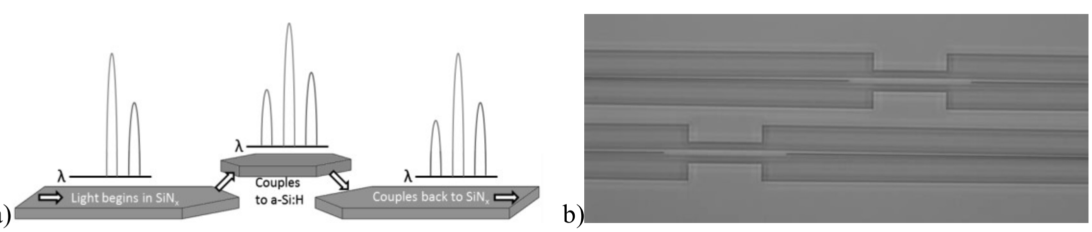

Figure 1. a) SiN_x to a-Si:H interlayer coupler design b) Optical microscope image of fabricated coupler.

We begin fabrication with a 100 mm silicon wafer with a 3 μm thick layer of thermal oxide on its surface. We first deposit 260 nm of low pressure chemical vapor deposition (LPCVD) SiN_x. Next, platinum alignment marks are patterned using electron beam lift-off lithography. We then write waveguides in the SiN_x layer by e-beam lithography and reactive ion etching, and clad them with plasma-enhanced chemical vapor deposition (PECVD) oxide. The oxide surface is planarized with chemical mechanical polishing, and we deposit 240 nm of a-Si:H by PECVD. Waveguides are again written by e-beam lithography and inductively coupled plasma etching. Finally, this top layer of waveguides is clad with PECVD oxide and individual chips are diced out of the wafer.

3. Experimental Results

We launch light into waveguides with lensed fiber edge-coupling into inverse nanotapers with matched mode areas. We measure propagation losses of -2.2 dB/cm and -11.2 dB/cm in the SiN_x and a-Si:H waveguides, respectively, and interlayer coupler loss per transition of -0.45±0.05 dB. The transition loss is larger than the simulated loss likely due to error in alignment between layers or deviation from the designed vertical gap between layers. Loss due to waveguides crossings are -0.003 dB in SiN_x passing under a-Si:H and -0.3 dB in a-Si:H passing over SiN_x. Crosstalk is -34.6 dB in SiN_x to a-Si:H, and -31.7 dB in a-Si:H to SiN_x.

We also demonstrate nonlinear phenomena in the a-Si:H layer of this device, in the form of pump-degenerate four-wave mixing (FWM). We measure this process in two a-Si:H segments of 1 mm and 4 mm length coupled from SiN_x, and in a 4.9 mm section of only a-Si:H for comparison. A plot of pump power and FWM efficiency is shown in Fig. 2a. While it is clear from this plot that at some pump power levels the solely a-Si:H waveguide can have better efficiency than the interlayer a-Si:H waveguides, Fig. 2b shows that for any given level of FWM efficiency, the interlayer a-Si:H waveguides always have superior power output due to better output coupling for the low-loss SiN_x output. This shows that an interlayer-based device can produce better results than a single-material device. Figure 2c shows the power dependence of the FWM interaction in the interlayer-coupled a-Si:H device.

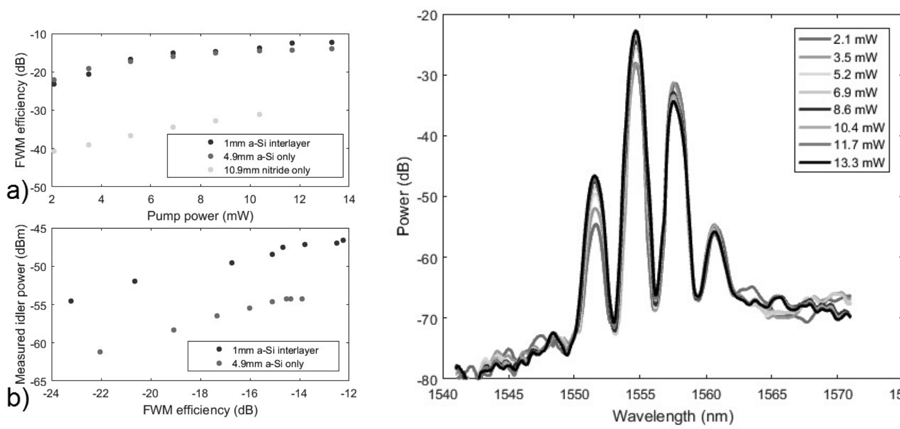

Figure 2. a) Average pump power plotted with FWM efficiency. b) FWM efficiency of a-Si:H waveguides plotted with measured idler power. C) FWM spectrum in the 1 mm a-Si:H interlayer waveguide.

4. Conclusion

In this work we demonstrate the first example of FWM through interlayer coupling between waveguides of SiN_x and a-Si:H. This enables a heterogeneous material platform capable of exploiting the best of both worlds in the tradeoff between propagation loss and nonlinearity. The platform can be extended to add more materials to add more device possibilities, which could eventually allow building an entire optical system on chip such as a quantum optical network. The 3D integration capabilities could also be useful for applications such as end-fire optical phased arrays.

References

1. J. F. Bauters, M. J. R. Heck, D. John, D. Dai, M. C. Tien, J. S. Barton, R. G. Heiderman, D. J. Blumenthal, and J. E. Bowers, "Ultra-low-loss high-aspect-ratio Si3 N4 waveguides," Opt. Express **19**, 3163–3174 (2011).
2. K. Ikeda, R. E. Saperstein, N. Alic, and Y. Fainman, "Thermal and Kerr nonlinear properties of plasma-deposited silicon nitride/silicon dioxide waveguides," Opt. Express **16**, 12987–21994 (2008).
3. K. Li, H. Sun, and A. C. Foster, "Four-wave mixing Bragg scattering in hydrogenated amorphous silicon waveguides," Opt. Lett. **42**, 1488–1491 (2017).
4. G. Roelkens, L. Liu, D. Liang, R. Jones, A. Fang, B. Koch, and J. Bowers, "III-V/silicon photonics for on-chip and intra-chip optical interconnects," Lasers Photonics Rev. **4**, 751–779 (2010).
5. J. Yao, X. Zheng, G. Li, I. Shubin, H. Thacker, Y. Luo, K. Raj, J. E. Cunningham, and A. V. Krishnamoorthy, "Grating-coupler based low-loss optical interlayer coupling," Group IV Photonics GFP 2011 8th IEEE Int. Conf. On (2011).
6. Y. Zhang, D. Kwong, X. Xu, A. Hosseini, S. Y. Yang, J. A. Rogers, and R. T. Chen, "On-chip intra- and inter-layer grating couplers for three-dimensional integration of silicon photonics," Appl. Phys. Lett. **102**, 211109 (2013).
7. R. Takei, Y. Maegami, E. Omoda, Y. Sakakibara, M. Mori, and T. Kamei, "Low-loss and low wavelength-dependence vertical interlayer transition for 3D silicon photonics," Opt. Express **23**, 18602–18610 (2015).
8. K. Shang, S. Pathak, G. Liu, S. Feng, S. Li, W. Lai, and S. J. B. Yoo, "Silicon nitride tri-layer vertical Y -junction and 3D couplers with arbitrary splitting ratio for photonic integrated circuits," Opt. Express **25**, 10474–10483 (2017).
9. K. Itoh, K. Yuki, Y. Hayashi, J. Suzuki, T. Amemiya, N. Nishiyama, and S. Arai, "Vertical trident coupler for 3D optical interconnection," Group IV Photonics GFP 2016 IEEE 13th Int. Conf. On 60–61 (2016).